2013-12-01

Second-Order Perturbation Analysis of the St. Venant Equations in Relation to Bed-Load Transport and Equilibrium Scour Hole Development

Frans Joseph Lambrechtsen
Brigham Young University - Provo

Second-Order Perturbation Analysis of the St. Venant Equations in Relation to Bed-Load Transport and Equilibrium Scour Hole Development

Frans Joseph Lambrechtsen

A thesis submitted to the faculty of
Brigham Young University
in partial fulfillment of the requirements for the degree of

Master of Science

Rollin H. Hotchkiss, Chair
Gustavious P. Williams
A. Woodruff Miller

Department of Civil and Environmental Engineering

Brigham Young University

December 2013

ABSTRACT

Second-Order Perturbation Analysis of the St. Venant
Equations in Relation to Bed-Load Transport and
Equilibrium Scour Hole Development

Frans Joseph Lambrechtsen
Department of Civil and Environmental Engineering, BYU
Master of Science

This analysis is an expansion of research done by Rollin Hotchkiss during his Ph.D work. The research uses fluid flow, sediment transport, and perturbation theory to predict where scour will occur in a variable-width channel. The resulting equations also determine equilibrium scour depth based upon the stream bed elevation derived from a dimensionless bed slope equation.

Hotchkiss perturbed the width of the channel using a second order Taylor Series perturbation but neglected second order terms. The present work follows the same procedures as Hotchkiss but maintains the second order terms. The primary purpose is to examine how the additional terms impact the final equilibrium scour depth and location results.

The results of this research show a slight variation from the previous work. With respect to a hypothetical case, there was not a significant amount of change, thereby verifying that scour migrates downstream with an increase in discharge. Interestingly, the comparison shows a slight increase in sediment discharge through the test reach analyzed. Supplementary to previous research, values of scour depth and location in terms of distance from the start of channel-width perturbation are provided; at the lowest discharge maximum scour occurs 4% of a wavelength upstream of the narrowest portion, and at the highest discharge maximum scour occurs at the narrowest point.

Additionally, a one-dimensional HEC-RAS sediment transport model and a two-dimensional SRH flow model were compared to the analytical results. Results show that the model output of the HEC-RAS model and the SRH model adequately approximate the analytical model studied. Specifically, the results verify that maximum scour depth transitions downstream as discharge increases.

Keywords: equilibrium scour depth, scour holes, saint venant, Reynolds transport theorem, bridge abutment, culvert, perturbation

ACKNOWLEDGMENTS

It is a pleasure to thank the many people who made this thesis possible. Foremost, I would like to express my sincere gratitude to my advisor, Dr. Rollin H. Hotchkiss, for the continuous support of my master's study and research, for his patience, motivation, enthusiasm, and immense knowledge. Throughout my thesis-writing period, he provided encouragement, sound advice, good teaching, and lots of good ideas. His guidance helped me in all the time of research and writing of this thesis. He believed in me when I didn't believe in myself; never told me that I should try something easier or simpler. I would also like to thank Dr. Gustavious P. Williams and Dr. A. Woodruff Miller for serving on my thesis committee; who patiently waited while I worked on my research.

I'd like to thank my friends the Roberts Family, my family, friends, and CH2M Hill who supported me in my desire to pursue a master's degree. Their constant enthusiasm, motivation, and kindness made all of this possible. I would have lost my mind without them. Additionally I would like to thank the administrative staff of the Civil and Environmental Engineering Department for befriending me and making me feel at home.

Finally, I would like to thank Brigham Young University and the "widow's mite" for making my education possible. Thank you!

TABLE OF CONTENTS

LIST OF TABLES

LIST OF FIGURES

1 INTRODUCTION

A major issue in stream channel design and management is scour hole development in critical reaches. Scour is due to stream discharge and channel geometry. Increases in scour have become a key issue in recent years as land has become more industrialized, and peak discharges have increased as a result.

The purpose of this work is to develop an equation that will help predict the magnitude and location of scour for uniformly sized sediment in a channel. Using the St. Venant Equations, perturbation theory, and equations for roughness and sediment transport (Garde et. al, 1985), a second-order equation was developed that achieves this purpose.

Major contributions from this work include the expansion of the St. Venant equations with perturbation and sediment theory integration to the second-order; additionally, graphical illustrations of the dimensionless equations to visually identify the patterns of sediment degradation; and values for scour depth with respect to distance from the initiation of perturbation. In addition, the analytical solutions were compared to commonly used one-dimensional and two-dimensional numerical results.

The remainder of this paper is outlined in the following order: review of literature, methods, first-order analysis, second-order analysis, comparison to numerical models, discussion of results, and conclusions.

2 BACKGROUND AND LITERATURE REVIEW

2.1 Description

Sediment transport is the result of physical forces on a streambed. These physical forces are a function of channel flow, velocity, shear stress, and channel friction to name a few (Garde et. al, 1985). An important factor is stream width: as a channel constricts, the velocity increases and the streambed experiences more scour. As bridges are commonly built at river constrictions the prediction of scour is critically important.

2.2 Analytical Models

Analytical models are mathematical in nature and examine equations versus quantities and magnitude of data. These models identify a solution that fits with multiple cases and scenarios; a solution at any magnitude of discharge, any sediment size, geometric variation, channel characteristics, etc. Any set of values for flow, roughness, sediment size, will return the most accurate solution. Analytical models are preferred over numerical or empirical solutions, but are more difficult to develop. The purpose of an analytical model is to provide results that represent the actual physics of the problem, and results based on physics are more accurate.

Analytic models are ultimately restricted because of the difficulty in including all of the relevant parameters required for a full solution. Computers have become more readily available with faster processing speeds and the hydraulic community has all but neglected the idea of an analytical solution and moved toward empirical models such as finite-difference and finite-

element analyses. After a thorough review, only a few studies actually discuss analytic methods. Nevertheless, the glimpses into the physics of sediment transport afforded by analytic work make it useful to pursue.

The work in this research expands on that of Hotchkiss (1989) and will be described in more detail later. Two other pertinent studies are from Chalfen et. al (1986) and Berthon et. al (2012). Chalfen et. al use a similar approach to analyze the equilibrium scour problem, but did not use a perturbation method to analyze the effects of expansions and contractions. Instead, they used differential schemes to determine water surface elevations and depths, which ultimately cannot be used without considering sediment transport. Berthon et. al solve the St. Venant equations using a similar substitution of the continuity and sediment transport Exner equation into momentum, to solve for bed elevation based on velocity, gravity, and unit width sediment discharge.

2.3 Empirical Models

Models that examine an empirical approach to equilibrium scour depth are plentiful and very common among researchers examining this particular phenomena. Such approaches address the problem of equilibrium scour by collecting large amounts of data over defined and specified intervals. Models developed by Dey et. al (2004) say that equilibrium scour models should be run for at least 48 hours. Simarro et. al (2011) say that empirical models should be run for a duration of two weeks. Some researchers consider this is a significant variation but more importantly it demonstrates there are a variety of procedures to performing numerical data collection. While these models vary in duration, the intervals at which data is collected are similar with the first few days, but vary as time goes on.

Specifically, empirical studies relate equilibrium scour to field-collected data such as stream width and sediment size. Statistical tools are used to develop equations using a logarithmic or regression analysis to identify equilibrium scour depth and the time when equilibrium depth was achieved (Lagasee et. al, 2009). Resulting equations are important because they help predict scour-hole development both physically and dynamically. They can infer how long scour takes to develop, which can help with remediation plans and channel design near bridges and culverts.

2.4 Numerical Models

Two models in particular include a one-dimensional model called HEC-RAS that includes a sediment transport analysis, and a two-dimensional model called Sediment and River Hydraulics (SRH) that uses a finite-element analysis (Brunner, 2010, Lai, 2009). One-dimensional HEC-RAS models have been used in research and commercial use for years while two-dimensional models are becoming increasingly popular as computing power increases. Two-dimensional river models typically use vertically-averaged velocities and laterally non-uniform velocities to enable simulation of recirculating eddies and flow separation.

Numerical models are applied to very specific stream reaches for specific flow requirements and do not apply outside of the specified conditions. Analytic models can be used to explore more general conditions.

2.5 Integrated Studies

Integrated studies use an equation based on analytical theory, which is then altered by using empirical data to adjust the analytical equation to fit. Parameters are attached to the equation that alter the form to fit the plot, i.e. depth versus discharge. One such piece of literature by Jain et. al (1989) provides a guide for estimating degradation, while Godvindasamy (2008) examines the

effects of scour at bridges using a simple three phase procedure in combination with collected scour data to determine risk.

3 METHODS

3.1 Governing Equations

The purpose of this section is to present the one-dimensional governing equations for water and sediment transport. Equations are presented for the conservation of mass and momentum (St. Venant Equations), sediment transport, and roughness. A definition sketch is provided in Figure 1. See Appendix A for a list of all variables and definitions.

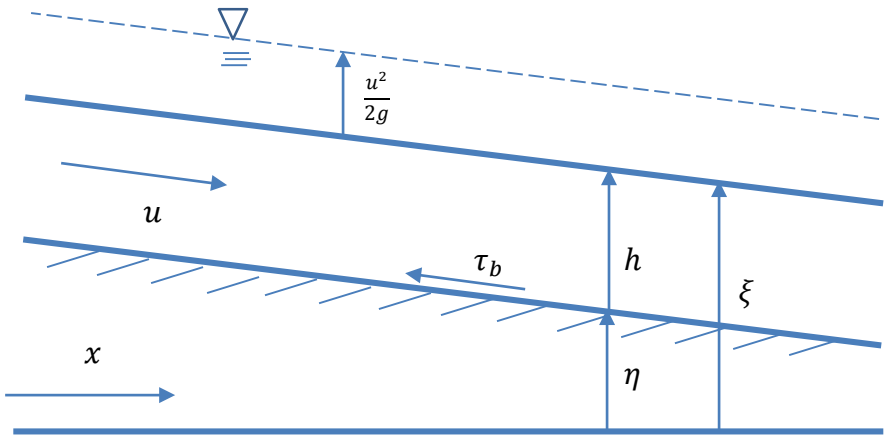

Figure 1. Definition sketch of theoretical channel. Parameters shown are bed elevation, water depth, velocity, bed shear stress, distance, velocity head, and water elevation.

With reference to the definition sketch in Figure 1, the St. Venant equations are:

$$Q = 2buh \tag{3.4}$$

$$\frac{d(u^2hb)}{dx} = -gbh\frac{\partial\xi}{dx} - bC_f u^2 \tag{3.3}$$

Where: $g = gravitational\ constant\ [LT^{-2}]$

$C_f = Darcy\ Weisbach\ friction\ factor\ for\ sediment\ [1]$

$b = channel\ half\text{-}width\ [L]$

$h = channel\ depth\ [L]$

$\eta = bed\ elevation\ [L]$

$\xi = channel\ depth\ plus\ bed\ elevation\ [L]$

$u = velocity\ [LT^{-1}]$

Simple power law function for sediment transport:

$$q_s = c_4 \tau_b^N \tag{3.5}$$

Where: $c_4 = generalized\ coefficien\ [T]$

$\tau_b = bed\ shear\ stress\ [mL^{-1}T^{-2}]$

$N = sediment\ transport\ exponent\ [1]$

Note the value N approaches a constant value as sediment transport increases (Garde et. al, 1985). The following is sediment continuity:

$$Q_s = 2bq_s \tag{3.6}$$

Where: $q_s = unit\ width\ sediment\ flowrate\ [mT^{-1}]$

Friction used is the Darcy Weisbach friction factor divided by eight (Whipple, 2004):

$$C_f = \frac{f}{8} \tag{3.7}$$

4 FIRST-ORDER LINEAR PERTURBATION OF ST. VENANT EQUATIONS

4.1 Discussion of Previous Work

The following is from Hotchkiss (1989). After some manipulation the governing equations are as presented in the following manner:

$$Q = 2uhb \tag{4.1}$$

$$\frac{d(u^2hb)}{dx} = -gbh\frac{\partial\xi}{dx} - bC_f u^2 \tag{4.2}$$

$$q_s = c_4\tau_b^N \tag{4.3}$$

$$Q_s = 2bq_s \tag{4.4}$$

The equations were made dimensionless using:

$\hat{b} = \frac{b}{b_o}$, $\hat{h} = \frac{h}{h_o}$, $\hat{S} = \frac{S}{S_o}$, $\hat{u} = \frac{u}{u_o}$, $\hat{Q} = \frac{Q}{Q_o}$, $\hat{Q}_s = \frac{Q_s}{Q_{s_o}}$, $\hat{q}_s = \frac{q_s}{q_{s_o}}$, $\hat{\xi} = \frac{\xi}{\xi_o}$, and $\hat{C}_f = \frac{C_f}{C_{f_o}}$.

Where the subscript refers to uniform channel and flow values.

The equations of motion then become:

$$\hat{h} = \hat{b}^{\frac{1-2N}{2N}} \tag{4.5}$$

$$\frac{d}{d\hat{x}}\left(\hat{u}^2\hat{h}\hat{b}\right) = \varepsilon\hat{S}\hat{b}\hat{h} - \varepsilon\hat{b}\hat{u}^2\hat{C}_f - F_{r_o}^{-2}\hat{b}\hat{h}\frac{d\hat{h}}{d\hat{x}} \tag{4.6}$$

$$\hat{S} = \hat{b}^{\frac{2N-3}{2N}} - \frac{1}{\varepsilon}\frac{d\hat{b}}{dx}\left(\frac{1-2N}{2N}\,F_{r_o}^{-2}\,\hat{b}^{\frac{1-4N}{2N}} - \frac{1}{2N}\,\hat{b}^{\frac{-1-N}{N}}\right) \tag{4.7}$$

Where: $F_{r_o} = Froude\ number$ [1]

$\varepsilon = \gamma C_f$ [1]

$\gamma = aspect\ ratio = \frac{b_o}{h_o}$ [1]

Hotchkiss used a perturbation analysis to determine the impact of a slightly varying-width channel on bed scour (see Figure 2). Neglecting any terms beyond the first-order, Hotchkiss found a linear solution. The dimensionless perturbed equations follow, with the hat-symbol dropped for simplicity.

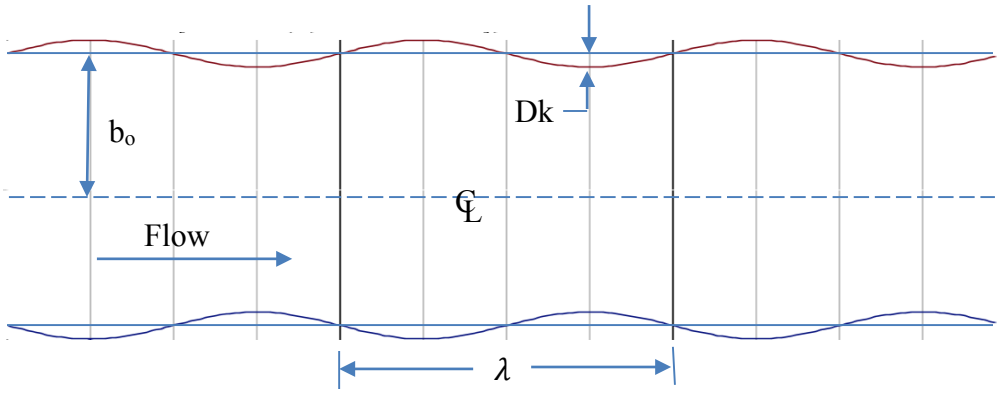

Figure 2. Plan view of hypothetical perturbed channel. Half width is displayed as well as perturbation amplitude and wavelength.

$$b = 1 + Dk\sin(kx) \tag{4.8}$$

$$k = \frac{2\pi b_o}{\lambda} \tag{4.9}$$

$$h = 1 + \omega\left(\frac{1-2N}{2N}\right) + \frac{\omega^2}{2}\left(\frac{1-2N}{2N}\right)\left(\frac{1-4N}{2N}\right) \tag{4.10}$$

$$S = 1 + \omega\left(\frac{2N-3}{2N}\right) + \frac{\omega^2}{2}\left(\frac{2N-3}{2N}\right)\left(-\frac{3}{2N}\right) + \frac{1}{\varepsilon}\frac{d\omega}{dx}\left(F_{r_o}^{-2}\left(\frac{1-2N}{2N}\right) + \omega\, F_{r_o}^{-2}\left(\frac{1-2N}{2N}\right)\left(\frac{1-4N}{2N}\right) - \frac{1}{2N} - \omega\,\frac{1}{2N}\left(\frac{-2-2N}{2N}\right)\right) \tag{4.11}$$

Where: $k = wave\ number\ [L]$

$\lambda = wavelength\ [L]$

$\omega = Dk\ Sin(k\ x)\ [1]$

$Dk = perturbation\ amplitude \gg 1\ [1]$

After applying the derivative and performing some substitution the final dimensionless first-order equations are:

$$h = 1 + Dk \sin(k\ x) \left(\frac{1-2N}{2N}\right) \tag{4.12}$$

$$S = 1 + Dk \sin(k\ x) \left(\frac{2N-3}{2N}\right) + \frac{1}{\varepsilon} Dk(k) \cos(k\ x) *$$

$$\left(F_{r_o}^{-2} \left(\frac{1-2N}{2N}\right) \left(1 + \omega \left(\frac{1-4N}{2N}\right)\right) - \frac{1}{2N} \left(1 + \omega \left(\frac{-2-2N}{2N}\right)\right)\right) \tag{4.13}$$

Hotchkiss then examined the combined impact of discharge and a perturbed channel width by finding the location of maximum scour for discharges corresponding to 50% exceedence, mean annual, and bankfull. The results will be shown later in the context of the second-order perturbation.

5 SECOND-ORDER NON-LINEAR PERTURBATION OF ST. VENANT EQUATIONS

5.1 Difference from Previous Work

The current analysis expands upon the work of Hotchkiss and proceeds to analyze the effects of additional terms in the equation (up to the second-order). Making the present analysis a second-order, non-linear perturbation of the St. Venant equations.

5.2 Equations

Performing the same Taylor series expansion on the channel half-width, and comparing to equations (4.10) and (4.11), additional terms were identified that were not included in Hotchkiss (1989). By adding these terms (as underlined) the dimensionless equations result in the following:

$$h = 1 + \omega\left(\frac{1-2N}{2N}\right) + \frac{\omega^2}{2}\left(\frac{1-2N}{2N}\right)\left(\frac{1-4N}{2N}\right) \tag{5.1}$$

$$S = 1 + \omega\left(\frac{2n-3}{2N}\right) + \frac{\omega^2}{2}\left(\frac{2n-3}{2N}\right)\left(-\frac{3}{2N}\right) + \frac{1}{\varepsilon}\,\varphi\left[\left(\frac{1-2N}{2N}\right)F_{r_o}^{-2}\left(1 + \omega\left(\frac{1-4N}{2N}\right) + \underline{\frac{\omega^2}{2}\left(\frac{1-4N}{2N}\right)\left(\frac{1-6N}{2N}\right)}\right) - \frac{1}{2N}\left(1 + \omega\left(\frac{-2-2N}{2N}\right) + \underline{\frac{\omega^2}{2}\left(\frac{-2-2N}{2N}\right)\left(\frac{-2-4N}{2N}\right)}\right)\right] \tag{5.2}$$

Where: $\varphi = Dk(k)Cos(k\,x)$

5.3 **Analysis**

Beyond analyzing the equations by hand, the equations were also put into the mathematics program Maple (a high-order mathematical analysis program) to visually identify mathematical patterns. Before equations could be visualized all independent variables required initial condition values for input. The same hypothetical data used by Hotchkiss was used for comparison purposes.

The data comes from a hypothetical case along the Minnesota River, near Granite Falls, Minnesota. The channel is assumed to have an initial half width of 40 m and a channel slope of 0.001. Other geometric data include the wavelength with a value of 800 m, perturbation amplitude of 0.1 (or 4 m), and bankfull depth of 1 m. The actual physical wavelength is altered because of equation (4.9); it is approximately 1150 m. This particular case is analyzed using a single sediment size of d_{50} = 0.45 mm. In addition, the same discharges are used to complete the analysis; 50% exceedance discharge, mean annual discharge, and bankfull discharge.

Based on this flow and geometric information, further data needed to be calculated, which Hotchkiss provides in his analysis. Using this geometric data and discharge information he determined the normal depth, discharge, velocity, Froude number, Darcy Weisbach friction factor, and the exponent N in the sediment transport equation for the three discharges to be analyzed. The following in Table 1, is a summary of this data.

Table 1. Input values for the hypothetical channel.

Flow Regime	Normal depth (m)	Discharge (cms)	Velocity (m/s)	Froude Number	Friction Factor (C_f)	Exponent N
50% Exceedence	0.21	7.1	0.42	0.3	0.0105	2.58
Mean Annual	0.43	22.4	0.65	0.32	0.009	2.58
Bankfull	1.04	135	1.62	0.51	0.0035	1.63

5.4 Results

The following figures were developed in Maple and are in the following order. They are representations of dimensionless depth (h), dimensionless slope (S), and dimensionless bed elevation (η), respectively. Figure 3 is dimensionless depth from equation (5.1) and Figure 4 represents the difference between the first-order and second-order functions.

Figure 3 represents the dimensionless depth of the hypothetical channel. As expected the depth begins at one, which represents the initial dimensionless conditions. As the channel widens, the depth decreases, and then increases as the channel contracts. At half of the wavelength the depth begins to increase and reaches its maximum near the point of contraction. A small difference is shown in Figure 4 between the first-order and second-order analyses. The second-order depth is greater near the contracted and expanded portions of the channel at $\frac{1}{4}\lambda$ and $\frac{3}{4}\lambda$. Between these positions the difference is zero, and dimensionless channel depth is the same.

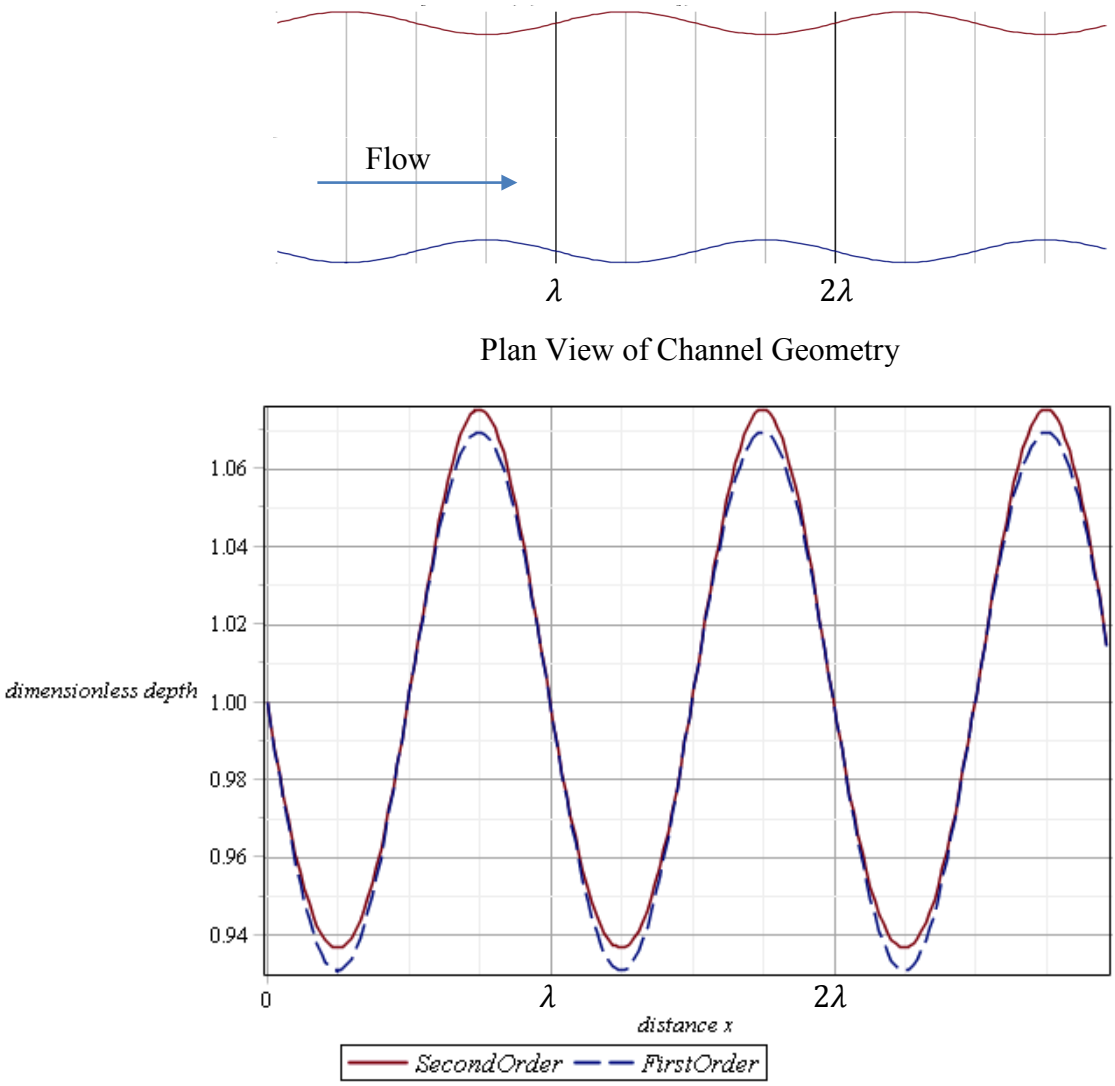

Figure 3. First and second order dimensionless water depth with respect to distance from start of channel perturbation. Y-axis is dimensionless and X-axis is in meters. Plan view of channel geometry is shown above for reference. Point of interest is channel contraction; occurs at $\frac{3}{4}\lambda$.

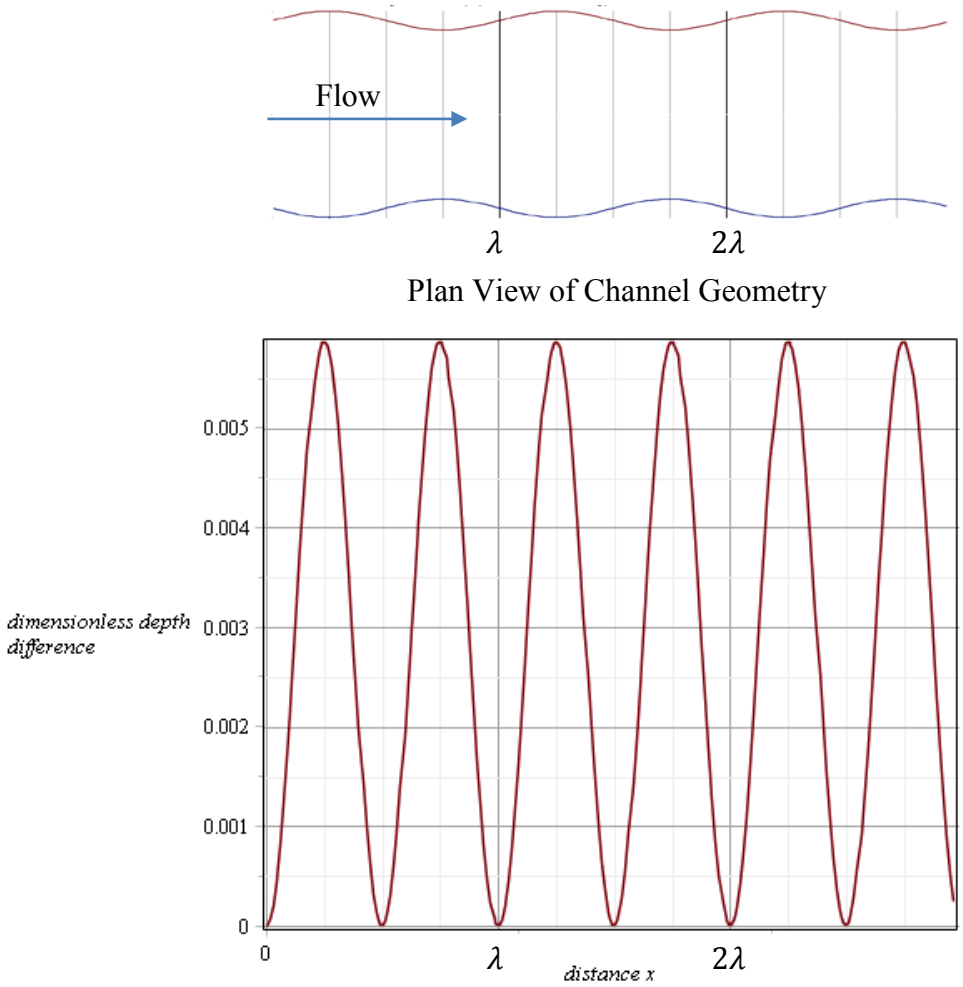

Figure 4. Difference between first and second order dimensionless water depth equations with respect to distance from start of perturbation.

A small variation from the first-order analysis is expected due to the additional terms in the second-order solution. This variation is hardly seen in Figure 5, of dimensionless slope from equation (5.2). Figure 6 shows the difference between the functions.

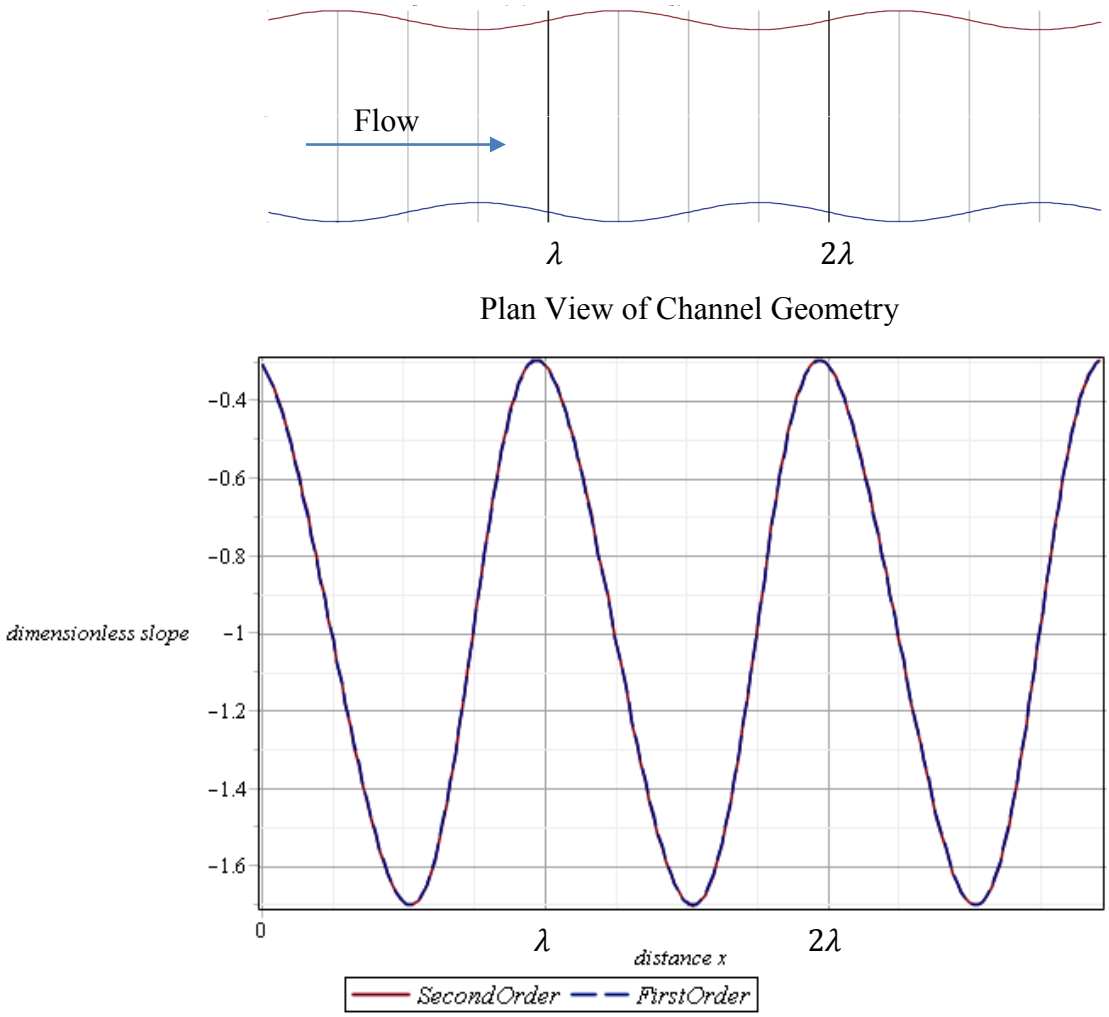

Figure 5. First and second order dimensionless bed slope equations with respect to distance from start of perturbation.

Dimensionless slope is shown in Figure 5. The place of interest for this plot is where the function crosses at a y-axis value of one; that is where the slope changes from a positive to negative, indicating scour. This change occurs near three-quarters of the wavelength.

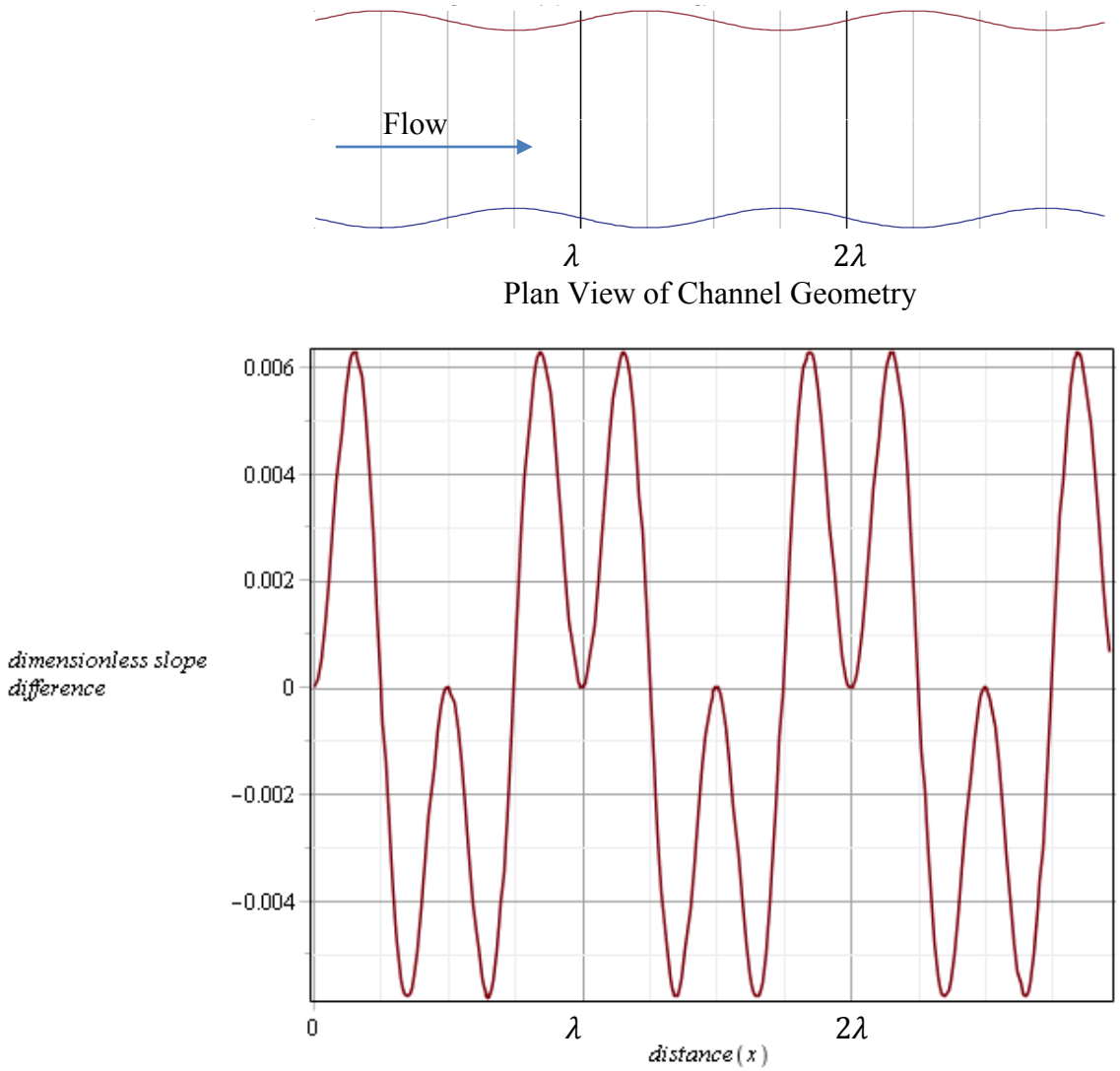

Figure 6. Difference between first and second order dimensionless slope equations with respect to distance from start of perturbation.

Figure 6 shows the actual difference between the first-order and second-order functions. There is very little variance shown between the two analyses performed. The max and min values are nearly the same and look almost identical. By integrating equation (5.2), the result is dimensionless bed elevation, which can be seen in Figure 7, with the difference between the functions shown in Figure 8.

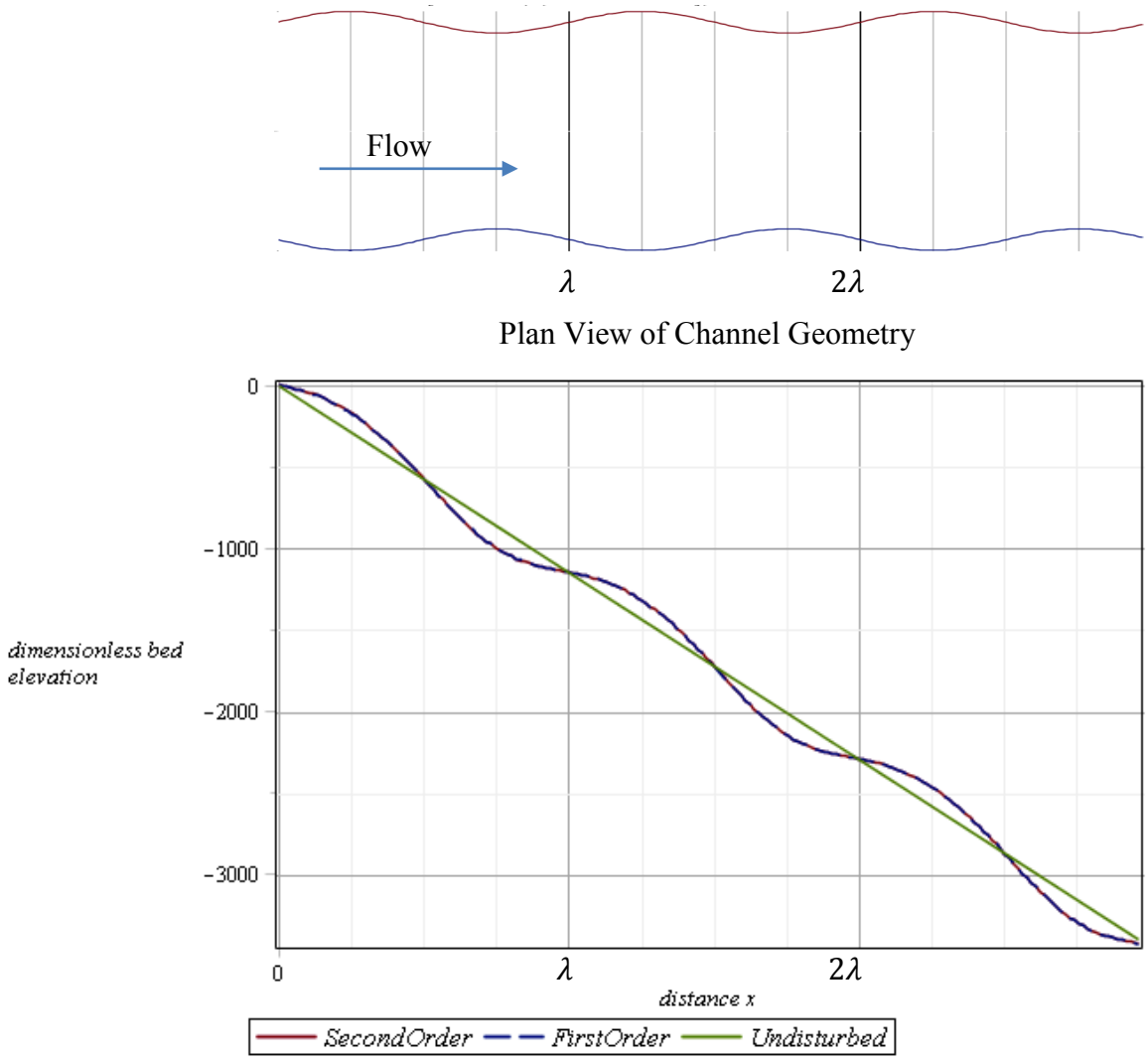

Figure 7. First and second order dimensionless bed elevation equations with respect to distance from start of perturbation. Unperturbed bed elevation is shown as a straight line.

Figure 7 shows the lowest bed elevation occurs around the same point of contraction as the previous figures, $\frac{3}{4}\lambda$. The undisturbed bed elevation is equal to the dimensionless slope value of one, and a line at a slope of negative one is displayed on the figure above to represent the undisturbed bed elevation.

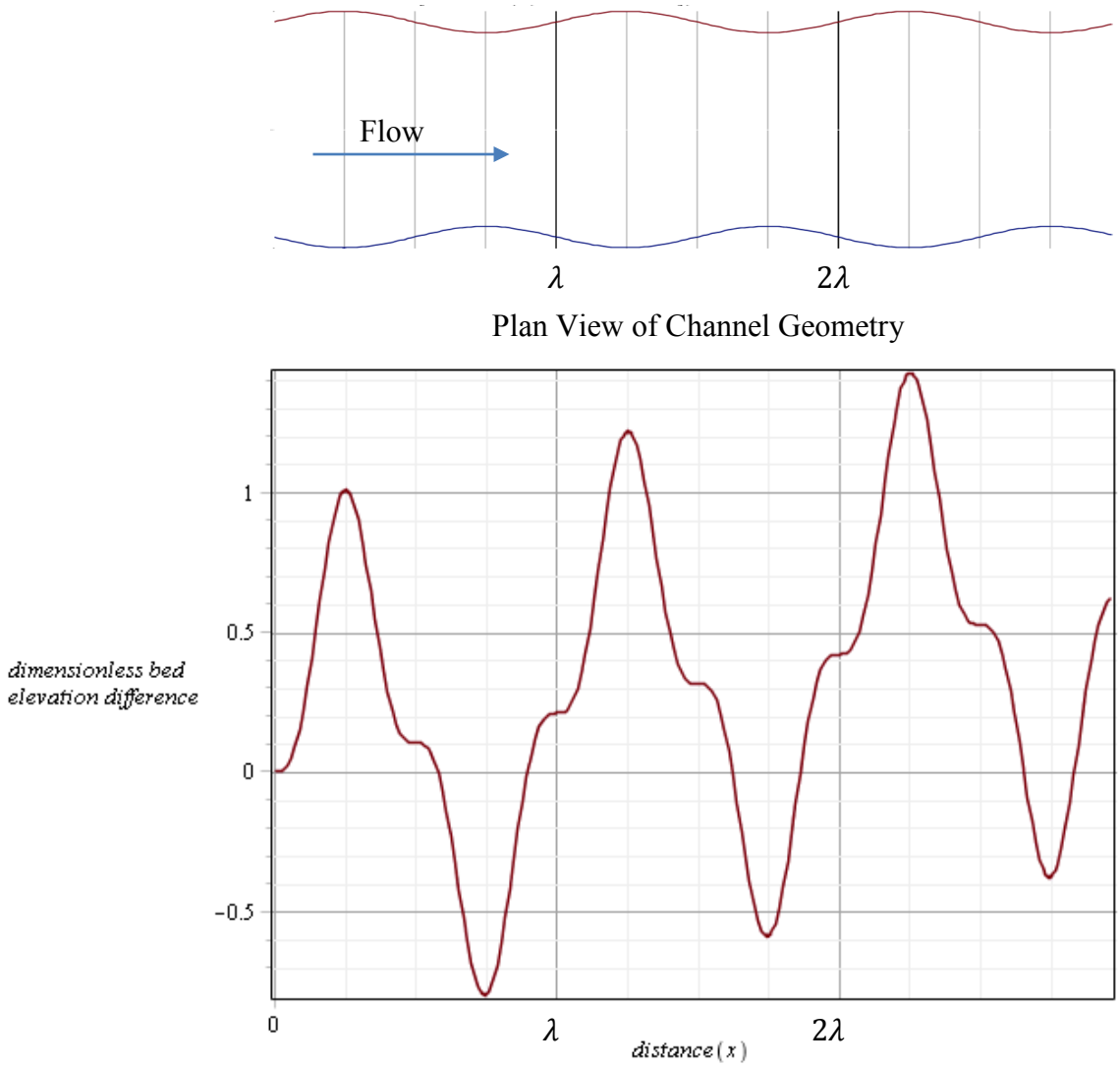

Figure 8. Difference between first and second order dimensionless bed elevation equations with respect to distance from start of perturbation.

It also shows where points of degradation and aggradation occur. Bed elevation for the first-order solution is nearly identical for the second-order case, as seen in Figure 8, and shows little difference between the two functions. The difference in bed elevation from the undisturbed channel can be determined by taking the difference between the undisturbed function and the first and second-order functions. This is graphically shown in Figure 9.

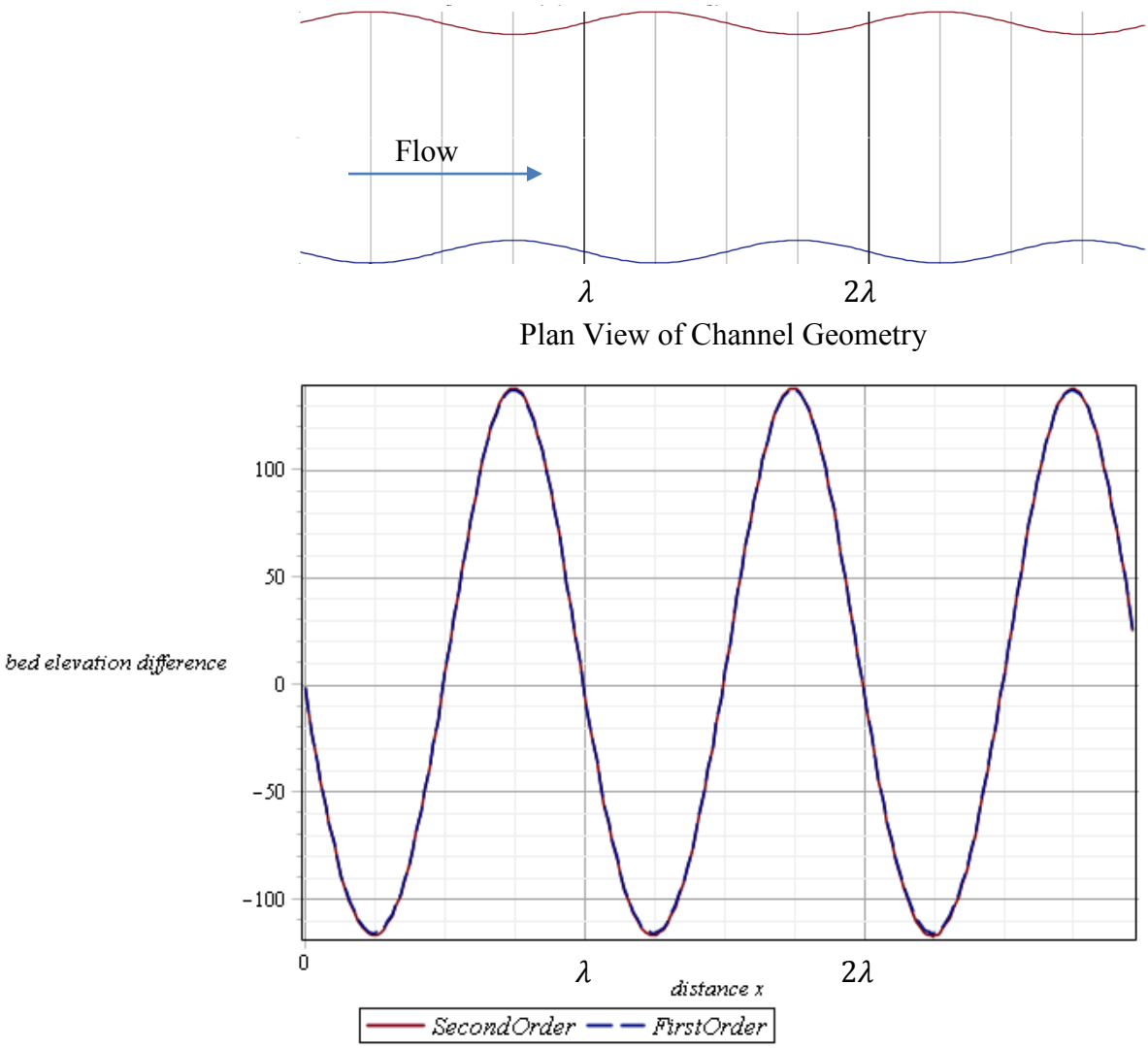

Figure 9. Difference between first and second order bed elevation equations and the unperturbed bed elevation. See Figure 7 for reference.

This plot is the difference between the undisturbed channel and the disturbed channel. The difference in bed elevation goes down at the widest portion of the channel, and later increases near the point of contraction. Where the difference equals zero is where the channel has returned to the original undisturbed bed elevation. Using this plot the distance where max scour depth can be identified.

The data shown in the Figures 3-9 uses bankfull discharge because it represents the most extreme case for potential scour. The discharge with respect to distance of scour and dimensionless scour depth, taken from these functions, can be seen in Table 2.

Table 2. Distance where max scour occurs from the start of perturbation. Narrowest point occurs at $\frac{3}{4}\lambda$.

Flow Regime	Discharge (cms)	Distance (m, wavelength)
50% Exceedence	7.1	814 $\left(\frac{2.84}{4}\lambda\right)$
Mean Annual	22.4	839 $\left(\frac{2.93}{4}\lambda\right)$
Bankfull	135	856 $\left(\frac{2.99}{4}\lambda\right)$

6 COMPARISON TO 1D AND 2D NUMERICAL MODELS

6.1 Scope of Computational Sediment Transport Analysis

Two numerical models were employed to compare to the analytic model. The most commonly used computational model in use today is HEC-RAS developed by the Hydrologic Engineering Center and the Army Corps of Engineers (Brunner, 2010). This is a one-dimensional model developed to analyze hydraulics in channels and matches the dimensions of this analytic study. Analytic results are also compared to those from Sediment and River Hydraulics (Lai, 2009). While this model does not yet include the ability to simulate sediment transport, it can still provide an interesting perspective by examining computed velocity and shear stress.

6.1.1 One-Dimensional Sediment Transport Analysis: HEC-RAS

HEC-RAS was first used on a uniform channel under steady state flow conditions. The model and roughness values were verified and calibrated using the normal depth from three uniform flow values, as seen in Table 1. Calibrated Manning's roughness coefficients were 0.027 for the first two flows, and 0.0197 for the bank full flow regime. Sediment transport was added to this uniform unperturbed channel and analyzed to make sure the channel did not undergo degradation or aggradation. Sediment input for sediment size is limited to inputting 100% passing for one size, and 0% passing for another. Therefore, using the available defined sediment sizes, a gradation of 100% passing 0.5 mm and 0% passing 0.25 mm was used to estimate a d50 of 0.45 mm, as defined by the analytical model. The duration for the model was initially set to two weeks.

Duration was later increased to four weeks to verify bed elevation. However bed elevation increased, indicating equilibrium scour had not been achieved. The final model run time was set to a time period of six months and equilibrium scour depth conditions were confirmed at three months.

A perturbed channel was added to the most downstream quarter of the reach defined, with the first three-quarters remaining an unperturbed channel to provide a steady flow of sediment into the perturbed portion of the channel for recharge. Initial perturbed runs were conducted under steady flow without a sediment transport analysis. The model was checked and normal depths were verified against the uniform flow values. Then the sediment transport component was added, analyzed, and manipulated to determine what these results mean and how to compare them against the analytical results. The same procedures for the unperturbed runs were used.

The first three-quarters of the reach is uniform and shows no change in bed elevation, as expected. Figure 10 shows the change in streambed elevation, zoomed-in on the last quarter of the reach, with flow from left to right.

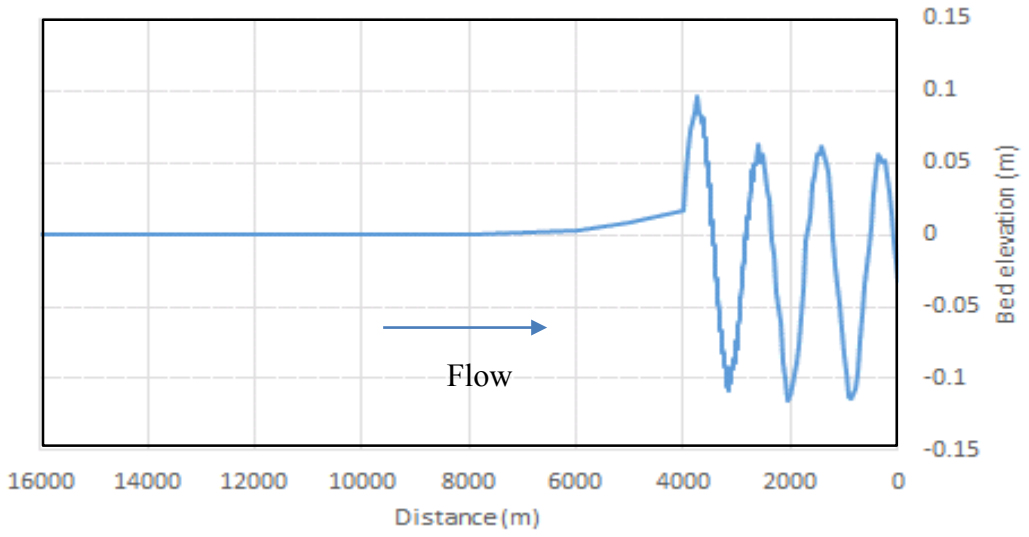

Figure 10. Change in bed elevation (y-axis) from HEC-RAS with reach distance in meters (x-axis).

Based on Figure 10, it appears the deepest point occurs around 3200 m from the end of the reach, with a scour depth of approximately -0.11 m. Table 3 shows the values of distance to scour from the start of perturbation (4000 m) and the scour depth in meters, with the analytical results.

Table 3. Data from HEC-RAS numerical analysis of distance and scour depth.

Flow Regime	Discharge (cms)	Distance			Scour Depth		
		Analytical (m)	HEC-RAS (m)	% Diff.	Analytical (m)	HEC-RAS (m)	% Diff.
50% Exceedence	7.1	814	740	6.46%	-0.029	-0.0058	80%
Mean Annual	22.4	839	800	3.40%	-0.061	-0.0348	43%
Bankfull	135	856	855	0.08%	-0.138	-0.109	21%

Looking at the values in the table, it appears the values follow a similar pattern as the analytical results, with the deepest scour depth occurring upstream of the narrowest portion, and nearest the contraction. As discharge increases the maximum scour depth approaches the narrowest portion of the channel.

An interesting piece of information was identified because of the numerical analysis. The max scour depth was observed over a time of approximately six months. This period was chosen after an iterative process of increasing the duration by weeks at a time to determine if equilibrium scour depth was achieved. Observing the data over each time step, the equilibrium scour depth appeared to be achieved after a time of three months. This is an interesting observation when compared to the discussion found in Simarro (2011), who estimates a duration of two weeks.

6.1.2 Two-Dimensional Sediment Transport Analysis: SRH

An identical model to the HEC-RAS model was developed using SRH. The same parameters, with three-quarters of the model being a uniform rectangular channel and the final quarter being a perturbed width portion, were used in conjunction with other characteristics. Model development began with a 2D-scatter set and was followed by a conceptual model to establish the boundaries of the mesh. Using the elevations prescribed in the scatter set, a mesh was interpolated resulting in triangular elements with quadrilateral nodes, with each node representing a point of calculation. Similar unto the HEC-RAS model, boundary conditions of steady flow were applied to the model at both the upstream and downstream ends of the mesh, with values of flowrate. Like the HEC-RAS model, the bed roughness values were calibrated using an iterative approach to values of 0.019 for the lower flows and 0.014 for bankfull. Flow depth was also verified against the values found in Table 1.

While sediment transport is not yet included in SRH, the 2D model can still provide insight that can be compared to the 1D model with respect to velocity magnitudes and bed shear stress values. Therefore the results of the two-dimensional model can still prove useful, even if the data comparison represents more of a strong relationship versus a confident interpretation.

Due to this limitation, only the SRH output for velocity and shear stress can be compared to HEC-RAS. Collecting the maximum values for bed shear stress and velocity from the SRH and HEC-RAS models, Table 4 and Table 5 compare the location and magnitude of these values.

Table 4. Max velocity comparison between HEC-RAS and SRH.

Flow Regime	Discharge (cms)	Distance			Velocity		
		HEC-RAS (m)	SRH (m)	% Diff	HEC-RAS (m/s)	SRH (m/s)	% Diff
50% Exceedence	7.1	933	931	0.17%	0.53	0.63	18.9%
Mean Annual	22.4	945	952	0.61%	0.85	1.05	23.5%
Bankfull	135	1005	1033	2.44%	1.71	1.75	2.34%

Table 5. Max bed shear stress comparison between HEC-RAS and SRH.

Flow Regime	Discharge (cms)	Distance			Bed Shear Stress		
		HEC-RAS (m)	SRH (m)	% Diff	HEC-RAS (N/m^2)	SRH (N/m^2)	% Diff
50% Exceedence	7.1	960	951	0.78%	1.88	2.12	12.8%
Mean Annual	22.4	960	976	1.40%	3.86	4.27	10.6%
Bankfull	135	1040	1036	0.35%	11.11	12.8	15.2%

Results show a strong correlation between the HEC-RAS and SRH, inferring if SRH included sediment transport, bed elevations would be similar results to HEC-RAS.

7 DISCUSSION OF RESULTS

7.1 Analytical Results

The analytical model identified in section 5 was plotted to identify the behavior of equilibrium scour depth. By collecting data from each flow regime the scour depth development pattern could be identified. In this case, the development of scour holes migrates downstream as discharge increases. This is similar to Hotchkiss' original results; he identified the max scour depth migrating downstream with increases in discharge, as seen in Figure 11. Using data from Table 2 and Table 3, distances of locations for max scour are shown on the figure, with an "A" indicating the second order analytical solution, "H" for HEC-RAS, and the number suffix indicating what case flow was used, with Case 1 being 7.1 cms, and Case 3 being 135 cms.

The location of maximum scour moves downstream, consistent with the results of the current analysis. The analytical results are clustered near the narrowest portion of the channel, while the HEC-RAS numerical results show a wider longitudinal distribution of max scour depth. In general, locations of max scour depth agree well with those from Hotchkiss' work.

The values in Table 2 are lower than expected; for an 80 m wide channel, to only obtain 14 cm (5.5 inches) bed elevation difference or scour is questionable. One explanation is the perturbation amplitude. If there is no perturbation then scour or change in bed elevation will not occur because sediment transport is uniform longitudinally and laterally across the reach; the greater the amplitude the greater the scour.

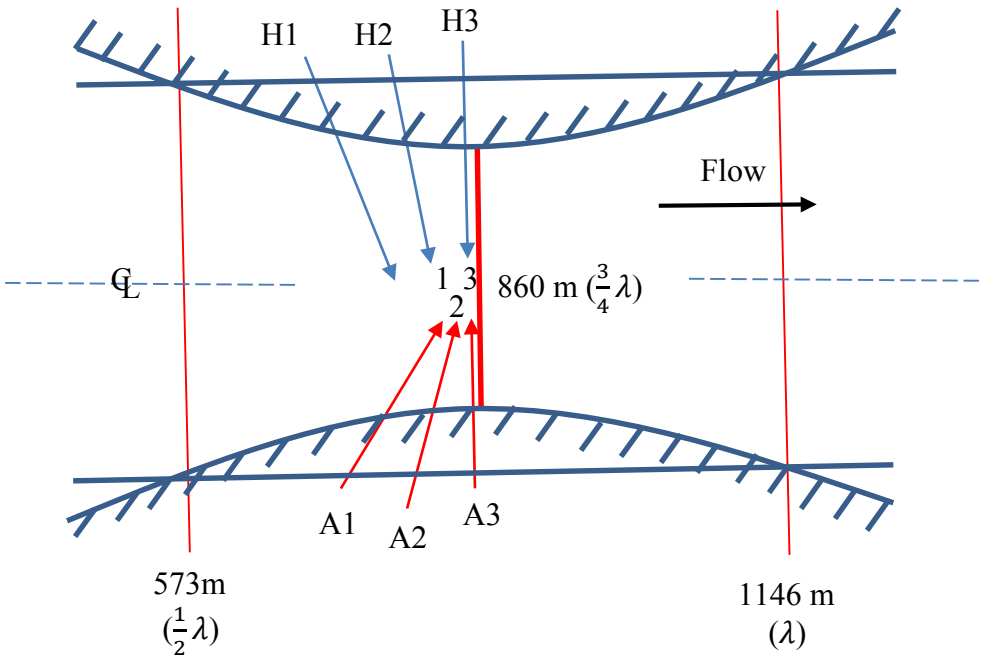

Figure 11. Comparison plot between the first-order equations, second-order equations, and HEC-RAS. Locations 1, 2, and 3 are locations of maximum scour from Hotchkiss (1989) analyzed at discharges of 135, 22.4, and 7.1 cms. Locations A1 and H1, A2 and H2, and A3 and H3 were analyzed at the same discharges of 1, 2, and 3 respectively. "A" refers to second-order analytic solution, "H" refers to HEC-RAS.

7.2 Comparison to Numerical Models

Results from the analytical model compare well to the numerical models. The scour depths identified in Table 3 show the same pattern of equilibrium scour magnitude migrating downstream towards the narrowest point in the channel width. The magnitudes themselves vary from -0.0058 to -0.138, with a maximum difference of 6.5% between analytic and numeric results. Considering this is a comparison between a numerical and analytical model, the difference seems reasonable.

The HEC-RAS model underestimates scour at low discharge rates. As discharge rates increase, where significant scour is expected, the numeric model more closely matches the analytical but still underestimates by a short margin. Assuming the analytical results represent the

physics correctly, results from the HEC-RAS model should be increased slightly to compensate, depending on the discharge.

8 CONCLUSIONS

8.1 Conclusions

The contributions of this research include an in-depth understanding of the first-order model to expand the study to include second-order terms that identified the minute differences from the previous results. Additional contributions comprise an evaluation of the max scour depth pattern, where results confirm maximum scour depth migrates towards the contraction as discharge increases. Lastly, widely used numerical models were compared to the analytical results to identify their compatibility and validity, concluding that one-dimensional numerical models agree well with analytic theory but slightly underestimate scour depth.

While the sediment transport and hydrodynamic community has trended towards numerical and finite difference/finite element solutions, this work provides interesting results when considering the analytical versus numerical consideration among researchers. While this work was comprehensive and identified interesting aspects of sediment transport and hydraulics, it could still be continued further.

Future research on this subject should include a study of a two-dimensional model that includes sediment transport, which may be SRH when it becomes Version 3 or another model in use at the time. Additionally, a two-dimensional analytical study could be developed to see how it compares to the one-dimensional results, and identify how additional velocity vectors affect scour results in multiple dimensions. Furthermore, research could be conducted using these same analytical theories to determine how bridge piers or other objects affect scour. Finally, the use of

a non-uniform bed-load sediment transport equation could be used to examine the variances in the analytical approach versus the numerical.

REFERENCES

Berthon, C., Cordier, S., Delestre, O., and Le, M. H. (2012). "An analytical solution of the shallow water system coupled to the Exner equation." Comptes Rendus Mathematique, 350(3–4), 183-186.

Brunner, G. W., CEIWR-HEC (2010). "HEC-RAS River Analysis System User's Manual Version 4.1." www.hec.usace.army.mil

Chalfen, M., and Niemiec, A. (1986). "Analytical and numerical solution of Saint-Venant equations." Journal of Hydrology, 86(1–2), 1-13.

Dey, S., and Barbhuiya, A. K. (2004). "Clear water scour at abutments." Water Management, 157(WM2), 77-97.

Garde. R.J., and K.G. Ranga Raju. (1985). "Mechanics of Sediment Transportation and Alluvial Stream Problems." New Delhi, India: Wiley Eastern Limited.

Govindasamy, A., Briaud, J., Chen, H., Delphia, J., Elsbury, K., Gardoni, P., Herrman, G., Kim, D., Mathewson, C., McClelland, M., and Olivera, F. (2008). "Simplified Method for Estimating Scour at Bridges." GeoCongress 2008, American Society of Civil Engineers, 385-393.

Hotchkiss, R. H. (1989). "Reservoir Sedimentation and Sediment Sluicing: Experimental and Numerical Analysis." University of Minnesota, Thesis of PhD.

Jain, S., and Park, I. (1989). "Guide for Estimating Riverbed Degradation." Journal of Hydraulic Engineering, 115(3), 356-366.

Jaramillo, W., and Jain, S. (1984). "Aggradation and Degradation of Alluvial-Channel Beds." Journal of Hydraulic Engineering, 110(8), 1072-1085.

Lai, Y. (2009). "Two-Dimensional Depth-Averaged Flow Modeling with an Unstructured Hybrid Mesh." Journal of Hydraulic Engineering, 136(1), 12-23.

Lagasse, P.F., Clopper, P.E., Pagán-Ortiz, J.E., Zevenbergen, L.W., Arneson, L.A., Schall, J.D., and Girard, L.G.. (2009). “Bridge Scour and Stream Instability Countermeasures: Experience, Selection, and Guidance Volumes 1 & 2 Third Edition.” Federal Highway Administration. http://www.fhwa.dot.gov/engineering/hydraulics/.

Simarro, G., Fael, C. M. S., and Cardoso, A. H. (2011). "Estimating Equilibrium Scour Depth at Cylindrical Piers in Experimental Studies." Journal of Hydraulic Engineering, 137(9), 1089-1093.

Van Rijn, L. C. (1987). "Mathematical modeling of morphological processes in the case of suspended sediment transport." Delft Hydraulics Communication (382).

Whipple, K. (2004). "Hydraulic Roughness". 12.163: Surface processes and landscape evolution. MIT OCW.

APPENDIX A. LIST OF TERMS

Here is a detailed list of the variables used in the governing equations and their meaning:

$A = cross\ sectional\ area\ [L^2]$

$b = channel\ halfwidth\ [L]$

$C_f = Darch\ Weisbach\ friction\ facter\ divided\ by\ 8\ [1]$

$c_4 = generalized\ coefficient\ for\ sediment\ transport\ [T]$

$D(k) = channel\ width\ amplitude\ [1]$

$F_{r_o} = Froude\ number\ [1]$

$g = gravity\ constant\ [LT^{-2}]$

$h = channel\ depth\ [L]$

$k = wavenumber = \frac{2\pi b_o}{\lambda}\ [1]$

$n = force\ normal\ to\ surface\ [mLT^{-2}]$

$N = exponent\ from\ sediment\ transport\ [1]$

$Q = flowrate\ [L^3T^{-1}]$

$q_s = unit\ width\ sediment\ flowrate\ [mL^{-1}T^{-1}]$

$Q_s = total\ sediment\ flowrate\ [mT^{-1}]$

$S = bed\ slope\ [1]$

$t = time\ [T^{-1}]$

$u = velocity\ [LT^{-1}]$

$V = volume\ [L^{-3}]$

$\gamma = aspect\ ratio = \frac{b_o}{h_o}\ [1]$

$\varepsilon = \gamma C_f\ [L]$

$\eta = bed\ elevation\ [L]$

$\lambda = perturbation\ wavelength\ [L]$

$\xi = channel\ depth\ plus\ bed\ elevation\ [L]$

$\rho = fluid\ density\ [mL^{-3}]$

$\tau_b = bed\ shear\ strength$

$\varphi = Dk\ (k)Cos(kx)[1]$

$\omega = perturbation\ parameter\ [1]$

$\hat{b}, \hat{h}, \hat{S}, \hat{u}, \hat{Q}, \hat{Q}_s, \hat{q}_s, \hat{\xi}, \hat{C}_f, etc. = dimensionless\ variables\ as\ listed\ above\ [1]$

APPENDIX B. ADDITIONAL REFERENCES

Akram Gill, M. (1987). "Nonlinear solution of aggradation and degradation in channels." Journal of Hydraulic Research, 25(5), 537-547.

Andreas, R., B, M. S., JØRgen, F., and Jess, M. (2005). "Numerical and experimental investigation of flow and scour around a circular pile." Journal of Fluid Mechanics, 534, 351-401.

Ash, B. (2008). "Numerical Modeling of Unsteady and Non-Equilibrium Sediment Transport in Rivers." Izmir Institute of Technology, Thesis of MS.

Begin, Z. e. B., Meyer, D. F., and Schumm, S. A. (1981). "Development of longitudinal profiles of alluvial channels in response to base-level lowering." Earth Surface Processes and Landforms, 6(1), 49-68.

Bejestan, M. S., and Hemmati, M. (2008). "Scour Depth at River Confluence of Unequal Bed Level." Applied Sciences, 8(9), 1766-1770.

Borghei, S. M. (2010). "Local scour at open-channel junctions." Journal of Hydraulic Research, 48(4), 538-542.

Briaud, J., Ting, F., Chen, H., Gudavalli, S., and Kwak, K. (2002). "Maximum Scour Depth around a Bridge Pier in Sand and in Clay: Are They Equal?" Deep Foundations 2002, American Society of Civil Engineers, 385-395.

Engelund, F., and Hansen, E. (1972). “A Monograph on Sediment Transport in Alluvial Streams.” Teknisk Forlag, Copenhagen.

Gill, M. A. (1983). "DIFFUSION MODEL FOR DEGRADING CHANNELS." Journal of Hydraulic Research, 21(5), 369-378.

Hong, J.-H., Goyal, M. K., Chiew, Y.-M., and Chua, L. H. C. (2012). "Predicting time-dependent pier scour depth with support vector regression." Journal of Hydrology, 468–469(0), 241-248.

Laucelli, D., and Giustolisi, O. (2011). "Scour depth modelling by a multi-objective evolutionary paradigm." Environmental Modelling & Software, 26(4), 498-509.

Lim, S., and Cheng, N. (1998). "Scouring in Long Contractions." Journal of Irrigation and Drainage Engineering, 124(5), 258-261.

Lu, J., and Shen, H. (1986). "Analysis and Comparisons of Degradation Models." Journal of Hydraulic Engineering, 112(4), 281-299.

Oben-Nyarko, K., and Ettema, R. (2011). "Pier and Abutment Scour Interaction." Journal of Hydraulic Engineering, 137(12), 1598-1605.

Pritchard, D. (2005). "On fine sediment transport by a flood surge." Journal of Fluid Mechanics, 543(00221120), 239-248.

Roulund, A., Sumer, B. M., FredsØE, J., and Michelsen, J. (2005). "Numerical and experimental investigation of flow and scour around a circular pile." Journal of Fluid Mechanics, 534, 351-401.

Sturm, T., and Janjua, N. (1994). "Clear-Water Scour around Abutments in Floodplains." Journal of Hydraulic Engineering, 120(8), 956-972.

Termini, D. (2011). "Bed scouring downstream of hydraulic structures under steady flow conditions: Experimental analysis of space and time scales and implications for mathematical modeling." CATENA, 84(3), 125-135.

Vasquez, J. A., Millar, R. G., and Steffler, P. M. (2007). "Two-dimensional finite element river morphology model." Canadian Journal of Civil Engineering, 34(6), 752-760.

Yang, J., Zhang, D., and Lu, Z. (2004). "Stochastic analysis of saturated–unsaturated flow in heterogeneous media by combining Karhunen-Loeve expansion and perturbation method." Journal of Hydrology, 294(1–3), 18-38.

Zhang, H., and Kahawita, R. (1987). "Nonlinear Model For Aggradation in Alluvial Channels." Journal of Hydraulic Engineering, 113(3), 353-368.